RADIO SCIENCE Journal of Research, NBS/USNC–URSI
Vol. 68D No. 4, April 1964

Lunar Semi-Diurnal Tides in $h'F$ and Their Influence on Transequatorial Radio Propagation

J. A. Thomas [1]

(Received Sept. 9, 1963; Revised Nov. 29, 1963)

The apparent partial dependence of anomalous transequatorial propagation on the phase of the moon has led to detailed investigation of the luni-solar tides in $h'F$ for 19 stations having magnetic dip values between +51° and −57°.

An attempt has been made to determine whether the computed tides were significant by means of power spectrum analysis. Significant large amplitude semi-diurnal tides were found only for regions near the magnetic equator at local solar times between 1900 and 2300 hours.

A propagation analysis has further shown that appreciable mode pattern changes with the changing phase of the moon are not to be expected for 16 Mc/s transequatorial propagation from Brisbane.

1. Introduction

For some years backscatter observations have been made at Brisbane of 16 Mc/s transequatorial radio propagation [Thomas, 1961; Thomas and McInnes, 1964]. A preliminary analysis of the recordings gave an indication that there might be some lunar influence on the propagation conditions. Thus, for example, the daily time of first observations of a particular anomalous echo appeared to be partially dependent on the phase of the moon.

Analysis of the various modes of propagation of 16 Mc/s signals traveling along great-circle paths from Brisbane has shown that the anomalous echo referred to above was due to reflections from the tilted ionosphere in the region of the early evening equatorial bulge. The most important single factor controlling the observation of such "tilt-mode" propagation appeared to be the height configuration of the ionosphere in the region within 2000 km of the magnetic equator. For this reason it was determined to carry out lunar tidal analyses of F region heights for a large number of stations in subtropical and tropical regions, in an attempt to delineate the height profile along various great-circle paths for various phases of the moon.

Unfortunately, the only height data readily available for such extensive analysis are the hourly values of $h'F$, and all the results of this work refer to such values. Table 1 lists the 19 stations for which analyses were carried out, together with the magnetic dip values and the periods analysed for each station.

Table 1

Station	Dip	Period analysed		Local solar times
		Years	Months	
Brisbane	−57°	1957, 58, 59	Nov.–Dec	1400–2100
		1958, 59, 60	Jan.–Feb	1400–2100
		1960	Aug.–Oct	12, 15, 16, 17, 20, 00
Tananarive	−55°	1956, 57	Nov.–Dec	1600–2300
		1957, 58	Jan.–Feb	1600–2300
		1959	Nov.–Dec	1600–1800
		1960	Jan	1600–1800
Townsville	−48°	1957, 59	Nov.–Dec	1500–2100
		1958, 60	Jan.–Feb	1500–2100
		1959	Aug.–Dec	1600–1800
		1960	Jan.–Dec	1600–1800
		1961	Jan.–July	1600–1800
Rarotonga	−40°	1956, 57	Jan.–Feb	1700–1900
		1956, 57	Nov.–Dec	1700–1900
		1957	Nov.–Dec	1500–2000
		1958	Jan., Feb., Nov., Dec	1500–2000

[1] Physics Department, University of Queensland; now at Physics Department (R.A.A.F. Academy), University of Melbourne.

TABLE 1—Continued

Station	Dip	Period analysed		Local solar times
		Years	Months	
Tahiti	−31°	1957	Dec	1600–2300
		1958	Jan.–Feb	1600–2300
		1959	Nov.–Dec	1800–2000
Buenos Aires	−31°	1958	Jan., Feb., Nov., Dec	1500–2000
		1959	Jan., Nov., Dec	1500–2000
		1960	Jan.–Feb	1500–2000
Lwiro	−30°	1953, 55, 57	May–Aug., Nov., Dec	1700–2300
		1954, 55	Jan., Feb., Nov., Dec	1700–2300
		1956, 60	Jan.–Feb	1700–2300
		1958, 59, 60	May–Aug	1700–2300
		1960	Jan.–Nov	1700–1900
		1960	Nov	1700–2300
Sao Paulo	−22°	1958, 59, 60	Jan.–Feb	1500–2000
		1957, 59	Nov.–Dec	1500–2000
Huancayo	2°	1957, 58, 59	Nov.–Dec	0000–2300
		1958	May–Aug	0000–2300
		1959, 60	Jan., Feb., May–June	0000–2300
Chimbote	6°	1957, 58	Nov.–Dec	1800–2200
		1958–59	Jan.–Feb	1800–2200
Djibouti	6°	1957	Nov.–Dec	1600–2300
		1958	Jan.–Feb	1600–2300
		1959	Nov.–Dec	1800–2000
Chiclayo	10°	1957, 58	Nov.–Dec	1700–2300
		1958, 59	Jan.–Feb	1700–2300
		1958	Nov.–Dec	1600
		1959	Jan.–Feb	1600
Talara	13°	1957, 58, 59	Nov.–Dec	1600–2300
		1960	Jan.–Feb	1600–2300
Dakar	17°	1956, 57	Nov.–Dec	1600–2300
		1957, 58	Jan.–Feb	1600–2300
		1959	Nov.–Dec	1800–2000
Baguio	19°	1957, 58, 59	Nov.–Dec	1400–2300
		1958, 59, 60	Jan.–Feb	1400–2300
Okinawa	36°	1957, 58, 59	Nov.–Dec	1500–2300
		1958, 59	Jan.–Feb	1500–2300
Panama	37°	1957	Nov.–Dec	0000–2300
		1958	Jan.–Feb	0000–2300
		1958	Nov.–Dec	1700–2300
Maui	40°	1957, 58, 59	Nov.–Dec	1500–2300
		1958, 59	Jan.–Feb	1500–2300
Puerto Rico	51°	1957	Nov.–Dec	1500–2300
		1958	Jan.–Feb	1500–2300

2. Data Selection

There have been a number of analyses made of tidal effects in the *F* region [Martyn, 1947, 1948; Burkard, 1948, 1951; Appleton and Beynon, 1948; McNish and Gautier, 1949; Eyfrig, 1952; Osborne, 1952; Baral, 1956; Brown, 1956; Yonezawa and Arima, 1958; Rastogi, 1961]: the majority of such analyses have been concerned with $foF2$ variations. Martyn [1947, 1948] and Brown [1956] showed that at two stations near the magnetic equator (Huancayo and Ibadan) there was a considerable luni-solar effect. This was particularly noticeable at Huancayo where the lunar tide in $h'F_2$ or $h_{\max}F_2$ was considerably greater in amplitude in the afternoon and early evening hours than at other times. Solar effects on the phase of the tides were also found. It was therefore considered necessary to carry out lunar analyses for a number of separate solar hours for the various stations, in order not to "smear out" any such luni-solar effect. The anomalous transequatorial propagation referred to above occurs almost entirely within the local Brisbane times of 1500 to 2300 hours; this then dictated the local times of interest in the analysis to be undertaken for each station.

Although there is a great paucity of suitable ionospheric stations in the Pacific area, Thomas and McInnes [1964] have shown that it is still possible to obtain reasonably correct information about the state of the ionosphere in this region by projecting data along either the lines of geomagnetic latitude or the lines of constant magnetic dip. Thus, for example, the measured value of $h'F$ for Talara (Dip $+13°$) at 2000 hours on a given day is assumed to be repeated at all points having the same dip value at the local time of 2000 hours for the point in question. It is necessary to determine the time difference between Brisbane local time and the local time at the intersection of each particular great circle path with the line of constant dip passing through the station being analysed. For this purpose charts similar to figures 1 and 2 have been prepared. Figure 1 enables the range (in a given direction from Brisbane) to any particular dip line to be determined, while figure 2 uses the range so determined to indicate the time advance (or delay) of the location with respect to Brisbane time. Thus a great circle path from Brisbane along a bearing of 50° (magnetic) will intersect the $+13°$ dip line (corresponding to Talara data) at a range of 6600 km; if the local time at Brisbane is 17 hours, then the local time at the point of intersection will be $17+3.3=20.3$ hours (fig. 2). The majority of local times analysed for the various stations were determined in this way for great circle path propagation to the northeast of Brisbane in the afternoon—this being the direction in which the anomalous propagation mode is most commonly observed. The time interval has been extended for some stations of particular interest, e.g., Huancayo.

For most stations the analysis has been confined to the months of southern summer (November to February), for 2 or 3 years, but again this period has been extended for certain stations, e.g., Townsville, Lwiro, and Huancayo.

3. Tidal Analysis and Significance Testing

In a period of 29.53 solar days (one lunar month), at any one meridian and local solar time, the moon will pass through all possible phases. For each station and solar hour the mean value of $h'F$ over each lunar month (actually 30 days) was subtracted from each hourly value, and the resulting daily departures arranged according to the age of the moon [Chapman and Bartels, 1940]. The mean variations over the period of analysis were then subjected to harmonic analysis in order to determine the semi-diurnal component of the lunar tide (24 lunar hours being equivalent to 29.5 solar days for the purposes of tidal analysis).

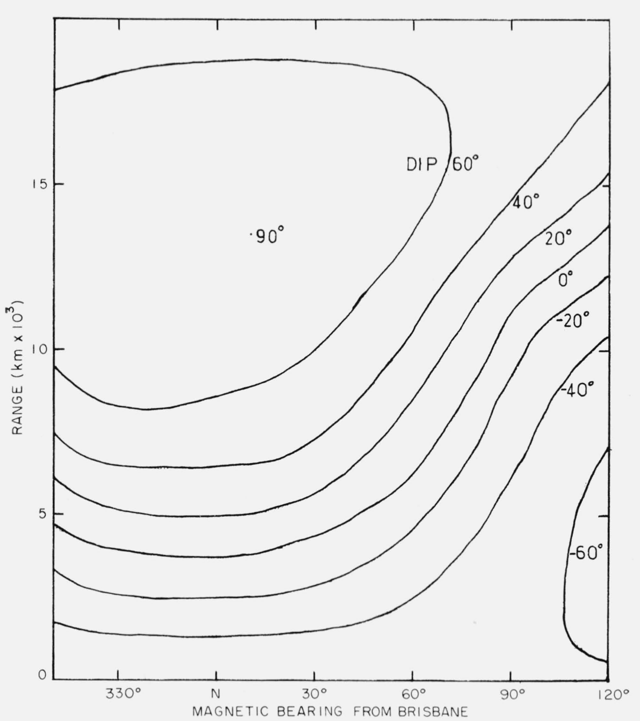

Figure 1. *Range—azimuth plots of magnetic isoclines as seen from Brisbane.*

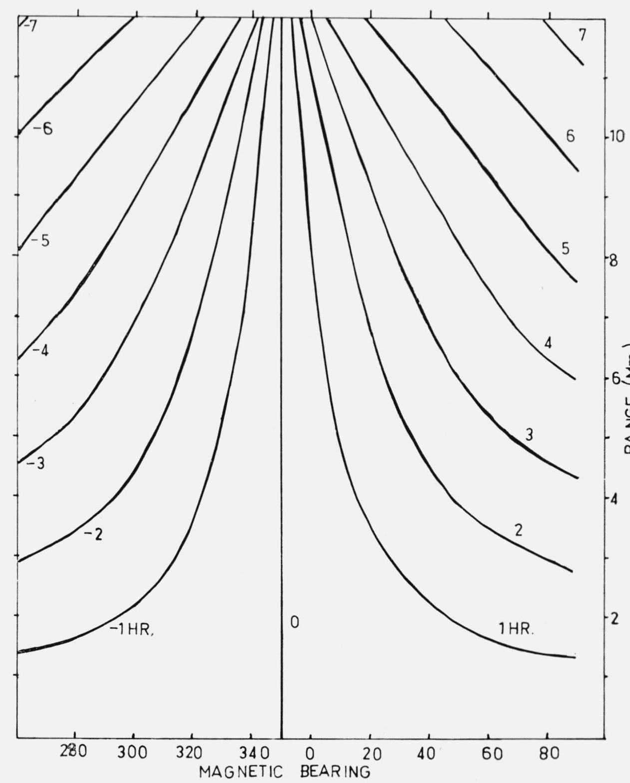

Figure 2. *Time differences for points at varying range and azimuthal bearing from Brisbane.*

The necessity for dividing the data into small groups for each solar hour and season leads of course to a considerable increase in probable error, and an attempt has been made to determine whether the lunar semi-diurnal tides extracted were significant or not. This was done, following Ward [1960] and Blackman and Tukey [1958], by computing the autocorrelation functions and power spectra of the data for a number of different locations and local solar times. Such an analysis gives an estimate of the strength of oscillations occuring in the data as a function of the frequency of oscillation, but gives no information regarding the relative phases of the component fluctuations. Limitations of sample size [2] mean that information is obtainable only at discrete intervals of frequency (or period) and a simple smoothing process, e.g., "hanning" [Blackman and Tukey, 1958], is often applied to the computed spectral estimates. On the assumption that sharp "lines" will not exist in the spectrum of the geophysical data analysed, a curve through such smoothed spectral estimates gives a first approximation to the oscillation strengths at periods between those actually computed.

In figures 3 to 6 are shown examples from two representative groups of smoothed spectral estimates (U_h) derived by the methods discussed by Blackman and Tukey [1958].

The first group (figs. 3 and 4) shows cases in which the previously derived lunar semi-diurnal tide is large. For certain solar times this is in fact the dominant periodicity present in the data. It must be remembered, however, that the oscillatory amplitude is the square root of the spectral power, so that in figure 3 for example, the 15 km ($\approx\sqrt{240}$) oscillation

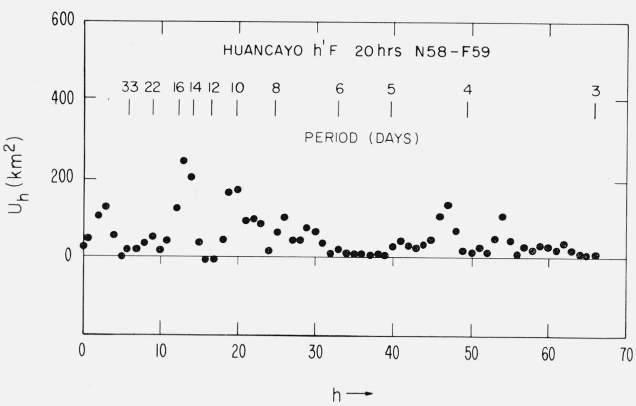

FIGURE 3. *Spectral estimates* (U_h) *of* h′F *values.*

[2] Because of the limitation of sample size, the largest run of daily values (for any one hour) used was normally only 120 days (four consecutive months). However, by combining data for several hours with closely similar tidal amplitudes and phases (e.g., 20, 21, 22 hours at Huancayo), it was sometimes possible to get effective runs of several hundred, and power spectra truncation lengths of either 60 or 100 days were used. Spectral "line powers" were available at periods given by

$$\text{Period (in days)} = \frac{2 \times \text{Truncation length (days)}}{\text{Frequency } h},$$

where h takes up integral values from zero to the number of sampling intervals in the truncation length. Estimates are not shown here for periods of less than 3 days.

with period 15 days is accompanied by a 13 km oscillation with period 10 days, as well as other smaller oscillations at higher frequencies. Probably the most outstanding feature common to the spectra of this group is the large amount of irregularity shown; this is partly associated with the small sample size used in the analysis. The absence of any consistent 27-day periodicity is also noteworthy.

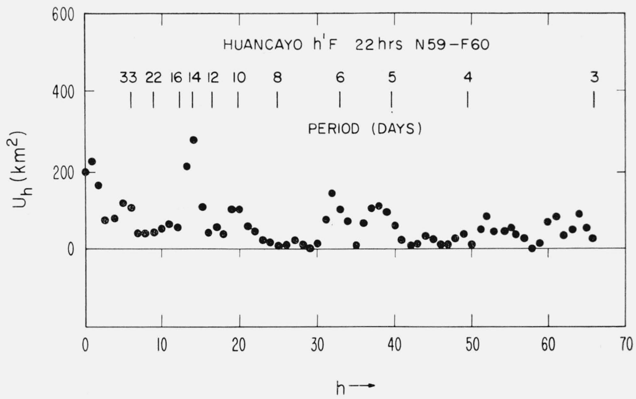

FIGURE 4. *Spectral estimates* (U_h) *of* h′F *values.*

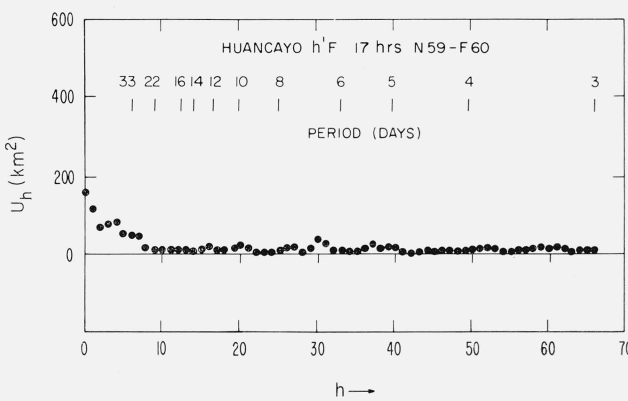

FIGURE 5. *Spectral estimates* (U_h) *of* h′F *values.*

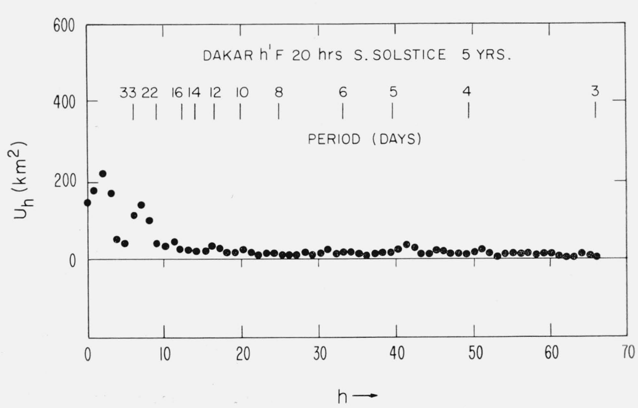

FIGURE 6. *Spectral estimates* (U_h) *of* h′F *values.*

The second group (figs. 5 and 6) contains examples of low spectral powers of lunar semi-diurnal period. There is generally much less irregularity in this group of spectra although the sample sizes are similar to those of the first group of *h′F* data. The cause of this difference probably lies in the fact that at the solar hours analysed in the first group, the ionosphere is very high and is rapidly changing in height, whereas the data used in the second group refer to solar times and localities at which this is not so.

Reasonable reliance may be placed on any lunar semi-diurnal tidal amplitude (and phase), only when the power spectrum for the corresponding data shows a reasonable peak (at period about 15 days) well elevated above the fluctuations due to the smallness of sample size. Thus the tides determined for the times and places of the first group may be regarded as being indicative of the presence of true semi-diurnal tides, although one might expect a fairly large probable error in the derived amplitudes and phases (e. g., 25% in amplitude).

Conversely, any tides derived for the times and locations of the second group must be viewed with suspicion. It should be stated that the lunar variations in starting time of observed anomalous trans-equatorial echoes fall into this group. The same is true also of the total duration and the strength of the anomalous TE echoes; the tidal effects first noted were apparently entirely fortuitous. In many cases of the *h′F* analyses, even when the spectral analysis indicated considerable doubt as to the validity of a given derived tide for a certain solar hour and location, it was often found that the amplitude and phase of the derived semi-diurnal tide showed quite smooth variations from one solar hour to the next. This presumably comes about because of the serial nature of the data used, and would probably arise in the Fourier analysis for other frequencies as well as that associated with lunar tides.

The general result appears that in a luni-solar analysis of the type attempted here, the only *h′F* tides that can be considered as definitely established are those in the immediate vicinity of the magnetic equator at solar times from 1900 hr to 2300 hr. Fortunately the computed tides are large only for those stations where they are considered to be well established, and the (magnetic) equatorial tides in fact dominate the scene so that the doubtful small amplitude tides do not materially effect the analysis presented below.

4. Analysis of Computed Semi-Diurnal Tides

For the local solar times of 1400 hr to 2300 hr the amplitude (P_2) and phase (t_2) of the lunar semi-diurnal tides, computed for the months of southern solstice (generally over 2, 3, or more years), are shown in ascending order of dip values in figure 7. Values of P_2 greater than 7 km occur only for the five stations with dip angle less than 13°, and then only for a few hours grouped about 2000 or 2200 hr. The four stations of the American chain (Huancayo, Chimbote, Chiclayo and Talara), show great similarity in both amplitude and phase variations, but the Djibouti data lead to somewhat smaller amplitudes, and a phase value of 10 hr rather than the 12 hr value shown at the American stations.

The magnitude and sense of the tidal displacement may be determined from the information given in figure 7 for each solar hour at each station for various phases of the moon. The results of such computations are shown in figure 8 for two different phases of the moon, viz, the moon 0 days and 4 days old. Because of the semi-diurnal nature of the oscillation the same two pictures will result approximately 15 days later, i.e., when the moon is aged 15 and 19 days respectively. Also, when the moon is aged 7 (and 22) days, the displacement will be the reverse

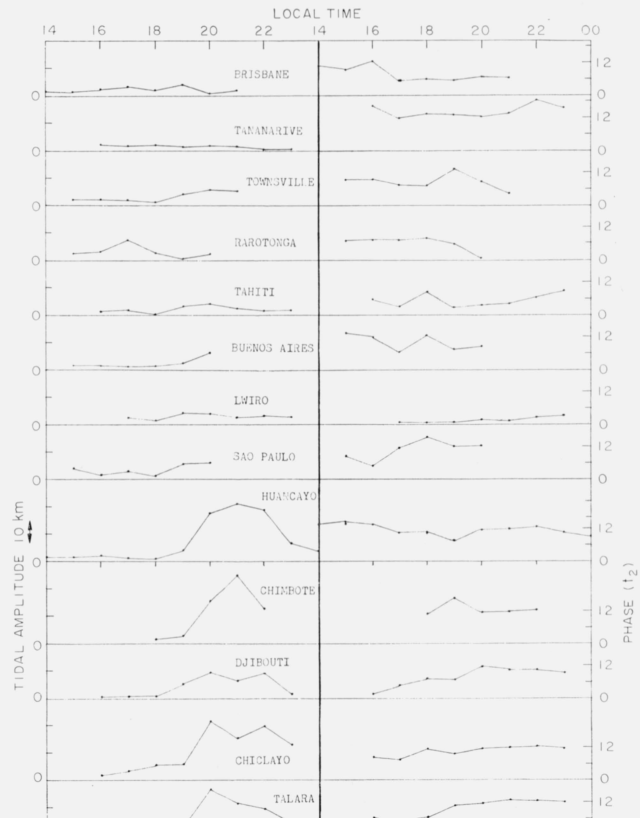

FIGURE 7. *Solar effects on the computed values of* P_2 *and* t_2 *lunar tides in* h′F.

Stations are arranged in order of increasing dip angle.

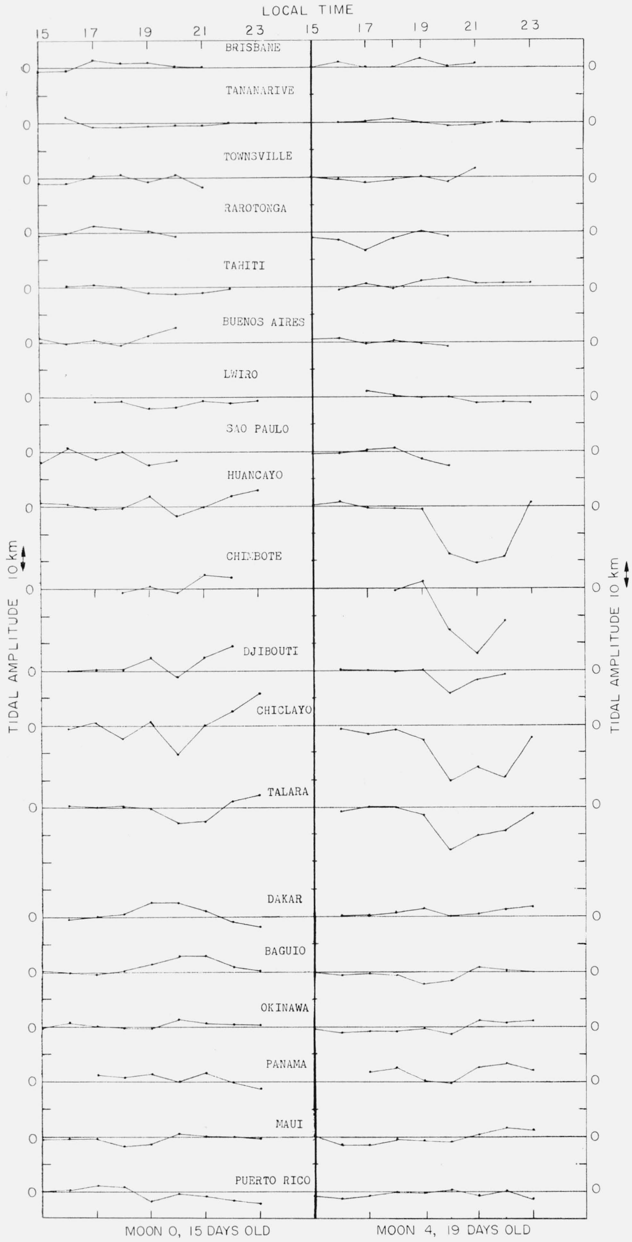

FIGURE 8. *Lunar semi-diurnal* h′F *tidal displacements for four phases of the moon.*

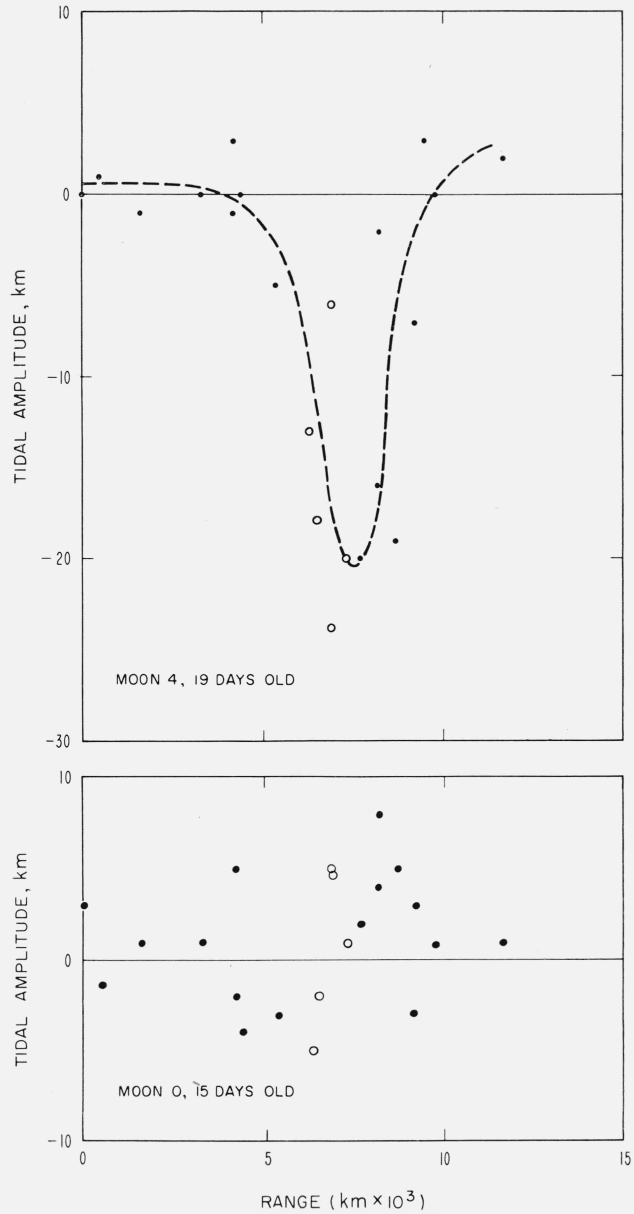

FIGURE 9. *Tidal displacements of* h′F *computed for four phases of the moon for a great circle propagation path leaving Brisbane on a bearing 70° Magnetic at 1700 hours in southern solstice.*

of that shown for age 0 days, and that for 11 (and 26) days will be the reverse of that shown for age 4 days.

By utilizing the data of figure 8, and the projection and timing methods outlined in section 2, it is possible to determine the tidal displacement (for a given phase of the moon) at various points along great-circle propagation paths from Brisbane. The values given in table 2 and plotted in figure 9 were derived in this way for propagation from Brisbane along a bearing of 70° (magnetic) at 1700 hr during the southern solstice. The points plotted as open circles in figure 9 are derived on the assumption that the tides have equal amplitudes and phases (at a given solar time) at points having the same *magnitude* of dip angle, irrespective of the sense of dip. These points fit reasonably well with the trends established by the solid points; more such points are not shown either because the range involved is too great (well beyond 10,000 km) or because tides have not been determined for the local solar times in question.

As might have been expected from the curves of figure 8, no significant tidal effect is found at times of new and full moon (and consequently also, none at times of first and last quarter when all semi-

TABLE 2. *Tidal amplitudes along a great circle path from Brisbane on a bearing of 70° M at 1700 hours in southern solstice*

Station	Range to interception with lines of constant dip	Local time	Amplitude at new moon	Amplitude when moon 4 days old
	km		*km*	*km*
Brisbane	0	1700	+3	0
Tananarive	500	1720	−1.5	+1
Townsville	1600	1800	+1	−1
Rarotonga	3300	1900	+1	0
Tahiti	4200	1940	−2	+3
Buenos Aires	4200	1940	+5	−1
Lwiro	4400	1950	−4	0
Sao Paulo	5400	2020	−3	−5
Huancayo	7700	2130	+2	−20
Chimbote	8200	2145	+4	−16
Djibouti	8200	2145	+8	−2
Chiclayo	8700	2200	+5	−19
Talara	9200	2220	+3	−7
Dakar	9500	2230	−3	+3
Baguio	9800	2240	+1	0
Okinawa	11700	2340	+1	+2
Panama	11900	2345		
Maui	12200	2350		
Puerto Rico	14100	0020		
−Huancayo	7300	2120	+1	−20
−Chimbote	6900	2100	+5	−24
−Djibouti	6900	2100	+5	−6
−Chiclayo	6500	2045	−2	−18
−Talara	6300	2040	−5	−13

diurnal displacements are reversed in sense from those observed at new and full moon).

However, at times when the moon is waxing crescent and waning gibbous (4 and 19 days old), a 20-km depression must exist in the height profile, with maximum depression occurring about 7500 km from Brisbane for the above path. An equal elevation will occur when the moon is waxing gibbous and waning crescent (11 and 26 days old). This will be true in general *for all propagation paths across the magnetic equator*—the height profiles will be elevated in the vicinity of the magnetic equator by up to 20 km at local times near 2100 hours (for the equatorial intersection), when the moon is approximately 11 or 26 days old, and depressed by the same amount when the moon is 4 or 19 days old.

By combining such derived tidal data with the mean $h'F$ profile for any month, the two extreme profiles may be obtained. Two examples are given in figure 10 for paths leaving Brisbane at 70° (magnetic) bearing in January 1961 at times of 1700 hours and 1500 hours respectively. It might be expected that such large distortions in the underside of the reflecting ionosphere would severely modify the propagation modes supported by the ionosphere. This supposition has been examined for 16 Mc/s

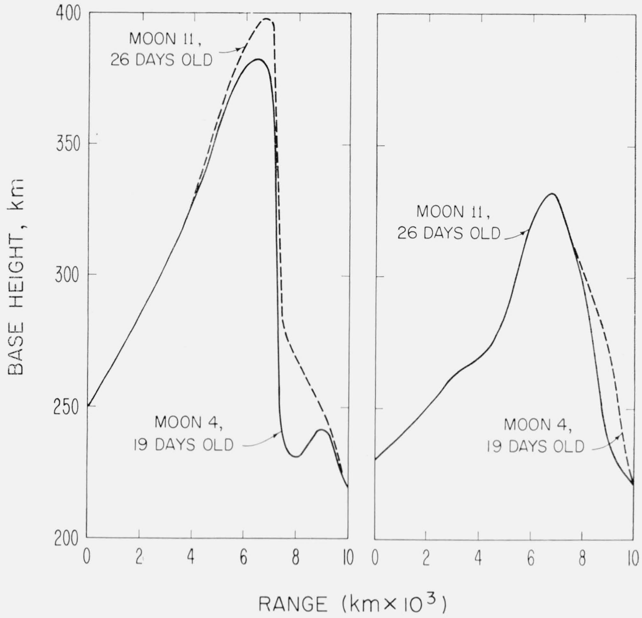

FIGURE 10. *Typical extreme* h′F *profiles for great circle propagation paths leaving Brisbane on a 70° Magnetic bearing at 1700 hours and 1500 hours in January 1961.*

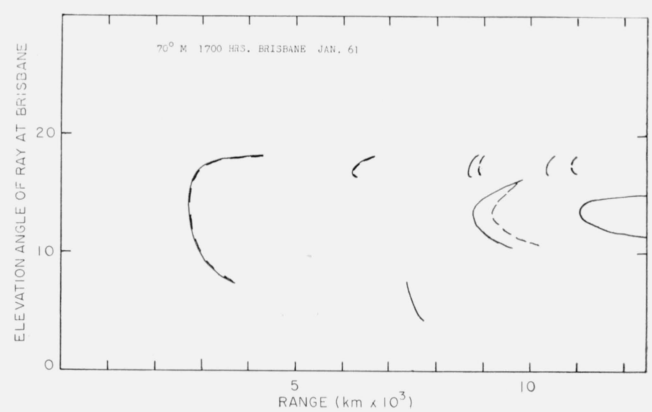

FIGURE 11. *Mode-angle plots for 16 Mc/s propagation from Brisbane in the specified direction at the times stated, showing the expected extreme changes due to semi-diurnal tides in* h′F.

Full lines correspond to the moon aged 4 or 19 days, and dashed lines to the moon aged 11 or 26 days.

signals by computing mode-angle diagrams [Kift, 1960] for several such profiles, utilizing the methods outlined by Thomas and McInnes, and assuming no tidal variations of f_0F_2. Figures 11, 12, and 13 give the results of three such analyses, where the solid lines refer to the situation when the moon is 4 or 19 days old, and the dashed lines, 11 or 26 days old. While there are certain differences, particularly in the higher order modes, these differences are not striking. It is therefore not so surprising that the observation of anomalous tilt-supported transequatorial propagation modes did not show any *significant* lunar tidal effects (see sec. 3).

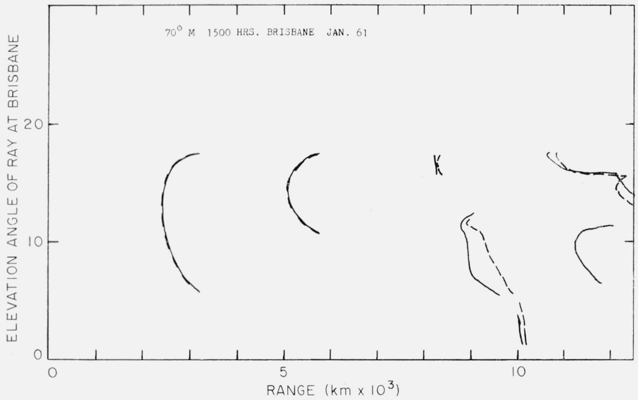

FIGURE 12. *Mode-angle plots for 16 Mc/s propagation from Brisbane in the specified direction at the times stated, showing the expected extreme changes due to semi-diurnal tides in* h′F.

Full lines correspond to the moon aged 4 or 19 days, and dashed lines to the moon aged 11 or 26 days.

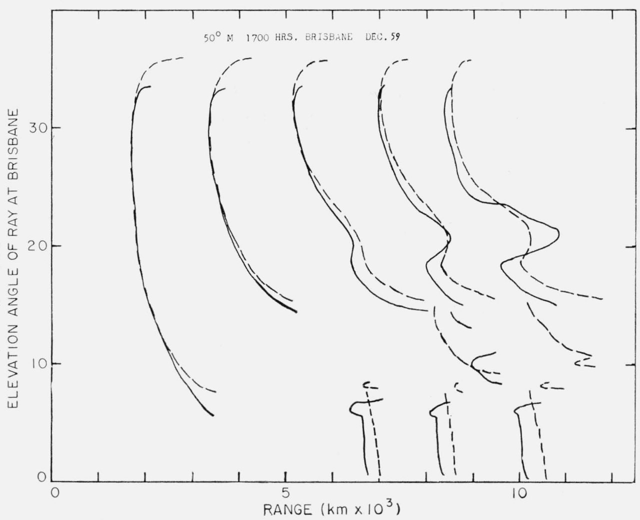

FIGURE 13. *Mode-angle plots for 16 Mc/s propagation from Brisbane in the specified direction at the times stated, showing the expected extreme changes due to semi-diurnal tides in* h′F.

Full lines correspond to the moon aged 4 or 19 days, and dashed lines to the moon aged 11 or 26 days.

5. Temporal Variations of Lunar Tides

As was mentioned in section 2, for certain stations, $h'F$ data was analysed for rather longer periods than most. The main features of these analyses are presented in figures 14 and 15.

Huancayo data analysed for three consecutive years (1957–9) for all solar hours during southern and northern solstices gave values of P_2 and t_2 as shown in figure 14. (The "summer" of the diagram refers to southern solstice.) A small seasonal effect is observable. The Panama data is for 1 year only and is of borderline significance. The Lwiro data, on the other hand, represents an average over 6 years for the solar hours in question, and the close similarity of summer and winter trends is noteworthy.

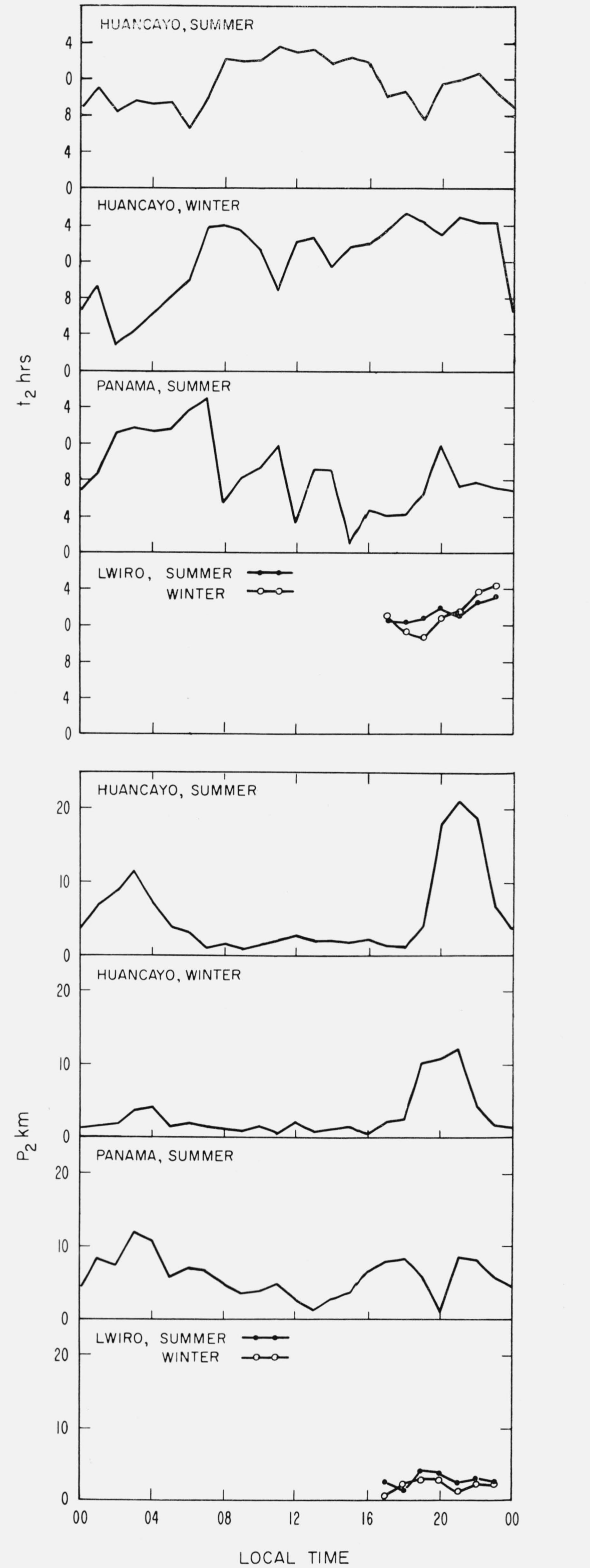

FIGURE 14. *Diurnal and seasonal variations in values of* P_2 *and* t_2 *for lunar tides in* h′F *at the stations specified.*

(Summer refers to southern solstice).

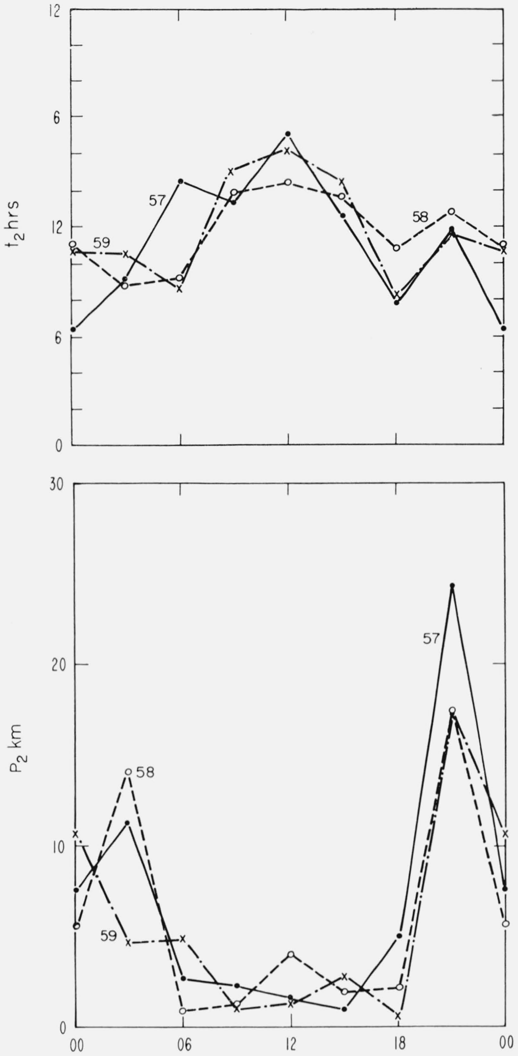

FIGURE 15. *Diurnal plots of* P_2 *and* t_2 *for Huancayo southern solstice values of* h′F, *showing the considerable degree of consistency from year to year.*

Figure 15 indicates for Huancayo southern solstice data, the close similarity in tidal amplitude and phase from year to year. (Three-hourly means have been plotted.) A more detailed analysis of the Huancayo and Lwiro tides determined over a reasonably large range of values of sunspot number, shows there is no significant change in the tidal amplitudes as a function of sunspot number. Such a change might possibly have arisen at Huancayo where it is probable that the (2000 hr) semi-thickness of the F layer varies considerably with sunspot number.

6. Conclusions

Although the original reason for investigating the effect of lunar tides on transequatorial propagation eventually proved to be trivial, it has been demonstrated that in the vicinity of the magnetic equator, large amplitude displacements of the virtual height of the F region will occur at definite phases of the moon, superimposed on the large height variations occurring from 1900 to 2300 hr local time. No significant lunar variation was found for $h'F$ values at stations with magnetic dip values greater than 20° in magnitude, nor for the equatorial stations outside the solar hours given above. This lack of significance may in part be due to data truncation.

This work, forming part of the general ionospheric research program of the Radio Research Board of Australia, was commenced in Brisbane and completed in Melbourne. The facilities of both the University of Queensland and the University of Melbourne have been made freely available and are greatly appreciated.

Particularly thanks are due to Professor H. C. Webster, Mr. M. J. Burke and the University of Queensland Computing Centre for their help and encouragement, to Mrs. D. Neilson for her assistance in data compilation, to Mr. B. A. McInnes for his assistance in analysing the various propagation modes, and Mr. P. Baker for carrying out the sunspot cycle analysis.

7. References

Appleton, E. V., and W. J. G. Beynon (1948), Lunar tidal oscillations in the ionosphere, Nature **162,** No. 4117, 486.

Baral, S. S. (1956), Lunar tidal variations in the F_2 region of the ionosphere, J. Technol. **1,** No. 2, 175–177.

Blackman, R. B., and J. W. Tukey (1958), The measurement of power spectra, Bell System Tech. J. **37,** 185–282.

Brown, R. A. (1956), Lunar variations of the F_2 layer at Ibadan, J. Atmos. Terr. Phys. **9,** No. 3, 144–154.

Burkard, O. (1948), Gezeiten in der oberen Ionosphare, J. Geophys. Res. **53,** No. 3, 273–277.

Burkard, O. (1951), Studie zum ionospharischen Gezeiteneffect. J. Atmos. Terr. Phys. **1,** No. 5/6, 349–352.

Chapman, S., and J. Bartels (1940), Geomagnetism, Oxford Univ. Press.

Eyfrig, R. (1952), Une influence lunaire sur e'altitude du centre de la couche ionospherique *F*2, C. R. Acad. Sci. Paris **235,** No. 14, 736–737.

Kift, F. (1960), The propagation of high frequency radio waves to long distances, Proc. Inst. Electr. Engrs. **107***B*, No. 32, 127–140.

McNish, A. G., and T. N. Gautier (1949), Lunar ionospheric variations at low latitude stations, J. Geophys. Res. **54,** No. 3, 303–304.

Martyn, D. F. (1947), Lunar tide variations in the *F* region near the magnetic equator, Proc. Roy. Soc. **190,** No. 1021, 273–288.

Martyn, D. F. (1948), Atmospheric Tides in the ionosphere; III. Lunar tidal variations at Canberra, Proc. Roy. Soc. **194,** No. 1039, 429–444.

Osborne, B. W. (1952), Lunar variations in the F_2 region critical frequency at Singapore, Nature **169,** No. 4303, 661.

Rastogi, R. A. (1961), The morphology of lunar semi-diurnal variations in *foF*2 near solar noon, J. Atmos. Terr. Phys. **22,** No. 4, 290–297.

Thomas, J. A. (1961), Transequatorial backscatter observation of magnetically controlled ionization, Nature **191,** No. 4790, 792.

Thomas, J. A., and B. A. McInnes (1964), in preparation.

Ward, F. W. (1960). The variance (power) spectra of Ci,Kp and Ap, J. Geophys. Res. **65,** No. 8, 2359–2374.

Yonezawa, T., and Y. Arima (1958), On the semi-diurnal lunar variations in the critical frequency, semi-thickness and height of maximum ionization of the *F*2 region in the daytime, J. Rad. Res. Lab. Japan **5,** No. 22, 303–314.

(Paper 68D4–357)